Towards Optimization of a Low Temperature Co-Fired Ceramic Catalyst Chamber for a Monopropellant Microthruster

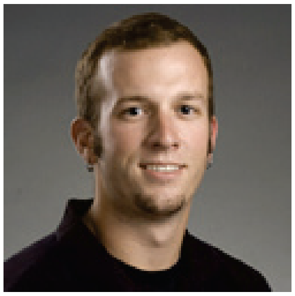

Andrew Vissotski: McNair Scholar

Dr. Don Plumlee: Mentor

Mechanical Engineering

Abstract

The reduction in space vehicle size and mass presents the need to develop a proportionally smaller propulsion system for orbital station keeping. A Low Temperature Co-Fired Ceramic (LTCC) monopropellant micropropulsion device has been developed at BSU. The simple, robust design features a heterogeneous catalyst chamber used to decompose a rocket-grade hydrogen peroxide monopropellant, to produce thrust. Initial prototype testing indicates only partial peroxide decomposition requiring an in-depth analysis of the geometric layout of the devices to increase system efficiency. This study employs a control volume based methodology to analyze the performance of various catalyst chamber designs. This approach was chosen due to the inaccuracies and difficulties associated with modeling the exact kinetics of a two-phase, catalytic reaction at the micro-scale. A full factorial experiment was established to investigate the effects of several geometries, typical to LTCC fluidics, on the hydrogen peroxide decomposition percentage. Chamber geometries were chosen based on previous thruster designs as well as constraints related to LTCC fabrication capabilities. Test results will determine which chamber designs to investigate in future optimization efforts. Reaction completion percentage and chamber temperatures are measured at steady state operation and used to compare the chamber geometries studied. Initial testing validated the accuracy and repeatability of the test apparatus. Mechanical failure of devices occurred during the transient start-up phase of device testing as a result of localized thermal expansion. A functional prototype was achieved by decreasing propellant flowrate and cross-sectional area reducing the released thermal energy. This lowered thermal stresses within the LTCC to a controllable level. Test results suggest three-dimensional fluidic channels produce higher decomposition percentages than similar configurations limited to a single plane.

Introduction

Background

The current trend in satellite design is the significant reduction in size and mass. The rapidly expanding field of Micro-Electro Mechanical Systems (MEMS) allows aerospace companies to minimize spacecraft volume without sacrificing function. This new breed of “micro-satellites” is defined as any spacecraft with a mass of 10-100 kg[1]. The smaller size offers a lower initial cost, increased redundancy and reduced launch costs. Single function, Micro-satellites will enable the deployment of clusters to replace larger traditional satellites, increasing the overall robustness of the system. For example, if a single micro-satellite were lost, the cluster would still retain most of its functionality.

The considerable decrease in satellite mass and volume presents new challenges to propulsion technology. Station keeping thrusters must also undergo a proportional reduction in size to maintain precise maneuverability. There are several micro-propulsion concepts currently being developed by aerospace companies and research universities to meet these requirements. These concepts are categorized according to propulsive energy type: electrical or chemical. Electric propulsion devices rely on the interactions between electrical and magnetic fields to accelerate particles to high velocities in order to produce thrust. The magnitude of thrust produced by this method is relatively low due to low mass flow rate of the fuel. In contrast, the specific impulse is usually very large for electrical propulsion devices due to the high exit velocities. Chemical thrusters utilize chemical reactions to convert propellant into thrust. A wide variety of potential propellants produce a wide range of chemical propulsion designs from solid rocket motors to liquid monopropellant and bi-propellant engines.

Each propellant type presents unique design challenges at the micro-scale. The liquid monopropellant concept is favorable due to its ability to be miniaturized without complexities associated with fuel/oxidizer mixing and ignition. It features a single propellant injected into a reaction chamber where it decomposes when in contact with a catalyst material. Additionally, cryogenic storage is not necessary because typical monopropellants are liquid at room temperature and atmospheric pressure. The most common monopropellants are hydrogen peroxide and mono-methyl hydrazine (MMH). The higher energy density of hydrazine is advantageous but its toxic exhaust products are a concern. The alternative hydrogen peroxide is considered a “green” fuel because it decomposes into a benign mixture of water vapor and oxygen when exposed to a catalyst[7]. Equation (1) describes the reaction for the catalytic decomposition of hydrogen peroxide.

$$2H_2O_2(l) \rightarrow 2O_2(g) + H_2O(g) + 23.44\ \text{kcal/mol} \qquad (1)$$

As with any chemical propellant, the degree and rate of reaction are directly related to the energy release. The ideal chemical propulsion device maximizes chemical energy released from the propellant in the shortest amount of time. This is also true of micro-propulsion devices. Propellant residence time, proper catalyst size coupled with chamber volume and enhanced heat loss associated with the small scale have been described by Kuan[5] and Platt[6] as major factors which greatly affect the decomposition efficiency. To improve decomposition rate within a catalyst chamber, a high catalyst surface area to chamber volume is preferred.

Motivation

Silicon MEMS thrusters have been developed and tested by Hitt, *et. al.*[2] that use of High Test Peroxide (HTP) as a monopropellant. These devices were fabricated using typical silicon MEMS fabrication techniques. The silicon MEMS fabrication process limits the device to a planar configuration. The silver catalyst was deposited onto the substrate with an aluminum shadow mask forming an array of diamond-shaped pillars within the catalyst chamber. Several of these cantilevered pillars failed during testing as shown in Figure 1. This presents questions regarding the structural integrity of silicon as a suitable material for micro-fluidic applications.

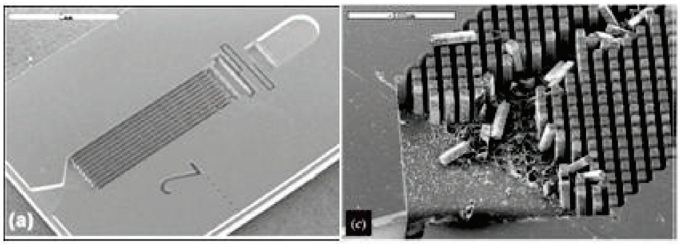

Figure 1. Silicon based HTP micro-thruster

Low Temperature Co-Fired Ceramics (LTCC) is an alternative material system available to the MEMS industry. LTCC has several advantages over silicon that make it a favorable material for MEMS applications, particularly monopropellant micro-thrusters. The compatibility with embedded silver catalyst and internal 3-D fluidic channel capability provides a wider range for catalyst chamber designs. The tolerance to high temperatures and high strength of LTCC are critical to developing a functional and durable monopropellant micro-propulsion device. One such micro-propulsion device is currently under development at Boise State University by Plumlee, *et al.*[3,4]. This device utilizes 90% HTP as a propellant to produce low levels of thrust for station keeping of micro-satellites. Four basic LTCC catalyst chamber designs were established and integrated with a previously developed converging-diverging nozzle. Each design features either a “Planar” or “3-D” concept as seen in Figure 2. This convention was established to describe the shape of the catalyst chamber channels. The term “3D” describes channels that transition vertically through the LTCC substrate by changing layers. Conversely, the term “planar” depicts a chamber design that remains in a single layer of LTCC. Silver is the preferred catalyst material for these thrusters and is deposited on the top and bottom surface of each embedded channel. A kinetic model of the catalytic reaction was established to determine the propellant residence time within the catalyst chamber. For a given volumetric flow rate, specified channel cross-section and predicted dwell time, a channel path length of 15 mm was determined to be used as a baseline reactor length and can be seen in Figure 2.

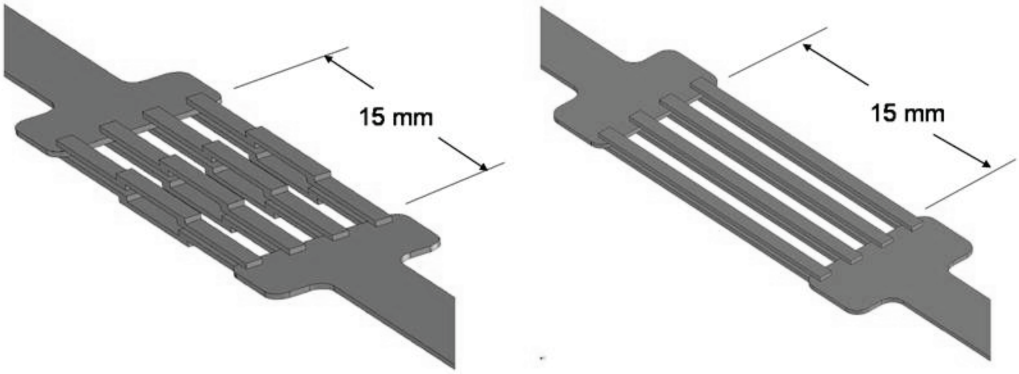

Figure 2. LTCC catalyst chamber concepts, “3-D” (left) “planar” (right)

Silicon and LTCC monopropellant micro-thruster designs are challenged by incomplete chemical decomposition, made evident by a visible exhaust plume during laboratory testing. Fuel efficiency is a vital operating parameter to spacecraft. Larger fuel efficiencies allow for lower volumes of propellant required for a particular mission. Future applications to micro-satellites demand optimizing thruster design to ultimately reduce costs and save space. Such a catalyst chamber is theoretically attainable and necessitates further investigation.

Methodology

Effective monopropellant decomposition is a complex phenomena that is difficult to model numerically. The coupled chemical kinetics and hydrodynamic behavior of the fluid within the catalyst chamber make theoretical and computational modeling extremely difficult at such a small scale[2]. The chemical kinetic model used to size the LTCC catalyst chamber assumed an isothermal reaction along the entire channel path length[3]. The propellant dwell time within the catalyst chamber was underestimated as a result of this assumption causing incomplete decomposition during laboratory tests. In an effort to increase LTCC micro-thruster performance, improvements to catalyst chamber design are under investigation at Boise State University. Proposed designs require experimental validation in order to accurately quantify their performance.

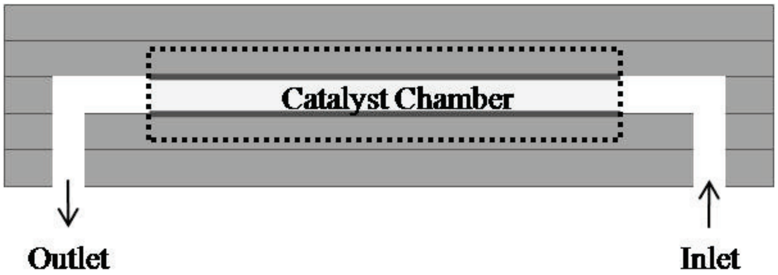

Figure 3. Schematic of LTCC catalyst chamber device

The scope of this work is to provide guidance for future optimization efforts of the LTCC monopropellant micro-thruster design. A control volume methodology was employed to analyze the performance of various catalyst chamber designs. Typical thruster components, such as the converging-diverging nozzle, are not the focus of this study and will not be integrated with prototype design. A conceptual device schematic is presented in

Figure 3. Catalyst chamber performance is quantified by full decomposition of the HTP entering the chamber. Therefore, incomplete decomposition can accurately be quantified by the *percent decomposition* defined in Equation 2, and used to compare competing designs. Where X_i is the concentration of HTP at the inlet and X_e is the mass fraction of hydrogen peroxide in the exhaust at the exit. A sample of chamber exhaust will be obtained and measured under steady operating conditions.

$$\% \text{ Decomposition} = 100*(X_i-X_e)/X_i \quad (2)$$

Dupont^{TM} 951 LTCC Green Tape was used exclusively for prototyping in this work. The current LTCC fabrication capabilities confine catalyst material deposition to the top and bottom channel surfaces. Device fabrication follows the C-MEMS procedure documented by Plumlee.[3,4] A CNC LASER mill was used to cut channel geometries into the Green Tape and a screen-printing technique was utilized to provide consistent silver paste deposition. Carbon tape was placed inside channels to ensure structural integrity during the 3,000psi lamination process. The stack of LTCC Green Tape layers sinter together when fired at 850°C, forming a uniform rigid body. The carbon placed inside each channel burns out during this process leaving internal fluidic channel with a rectangular cross-section. The LTCC material experiences shrinkage of ~14.5% along each axis. This is considered in the 3D design stage and all dimensions are scaled by a factor of 1.145 to compensate for shrinkage during firing.

To further reduce the variability between test devices, several parameters will be held constant. First, channel height is limited to a single layer of LTCC, totaling ~0.2 mm after firing. This provides a constant catalytic surface area to volume ratio within the chamber. Secondly, all prototypes will share a common cross-sectional area in order to assure the pressure drop is similar for each device. In addition, the total layers of LTCC per device will be the same to provide an equivalent thermal mass. Test substrate design, including embedded catalyst chambers exhibit symmetry about the device center to simulate equal thermal resistances allowing for heat generated from the reaction to dissipate evenly throughout the substrate.

Fluidic channels embedded in LTCC substrates feature several geometric characteristics that are unique to the material system. Several of these geometric factors, listed in the left hand column of Table 1, are thought to affect the catalyst chamber performance and are the primary focus of this study. They were selected based on previous micro-thruster designs featured in Figure 2.[3,4] A full factorial experiment was established to understand how each factor influences the decomposition of hydrogen peroxide. Each factor was assigned two values representing a range of potential values. The factors were limited to a "high" and a "low" value to reduce sample population. Three factors held at two discrete levels presents eight feasible combinations to be designed and tested.

Table 1. Experimental factors and corresponding levels

Factor Name	**Low**	**High**
Channel Shape	Planar	3-D
Path length	10 mm	20 mm
Number of Channels	2	6

The last factor listed in Table 1, "Number of Channels," is detailed in the cross-sectional view of Figure 4. Each prototype shares a common channel cross-sectional area and is restricted to a single layer of LTCC as seen in the figure. A cumulative channel width, *w*, is the only dimension required to design a multi-channel catalyst chamber. The individual channel width is simply a fraction of the total width. The fundamental difference between the low and high number of channels in Table 1 is the hydraulic diameter. It was decided that two and six channels represented an adequate amount of channel size variation to provide significant results without adding complexities to the fabrication process.

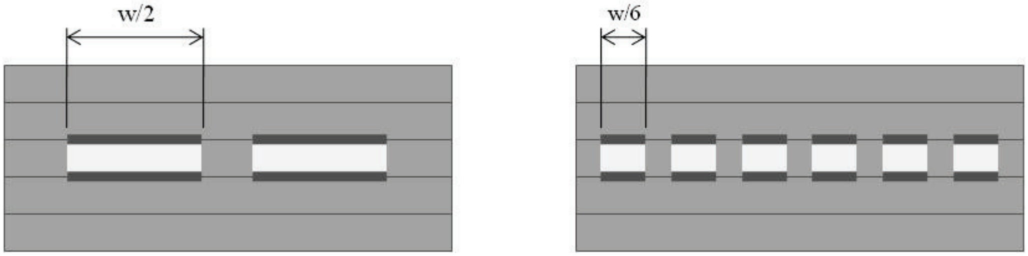

Figure 4. Cross-sectional view of LTCC prototypes illustrating "2 channels" and "6 channels"

“Channel shape” is hypothesized to be the most influential factor affecting catalyst chamber performance based on previous experimental testing. The 3D channel concept located at the top of Figure 5 is thought to enhance propellant mixing within the catalyst chamber caused by the abrupt vertical transitions between LTCC layers. The Planar channel configuration was proposed to illustrate any advantages or disadvantages inherent to the 3D configurations. “Path Length” describes the longitudinal distance covered by the silver catalyst, represented by solid black lines located on the top and bottom of the channel in Figure 5. The convention defines equivalent catalyst contact areas between planar and 3D configurations and can also be seen in the figure. This convention is followed for every design tested.

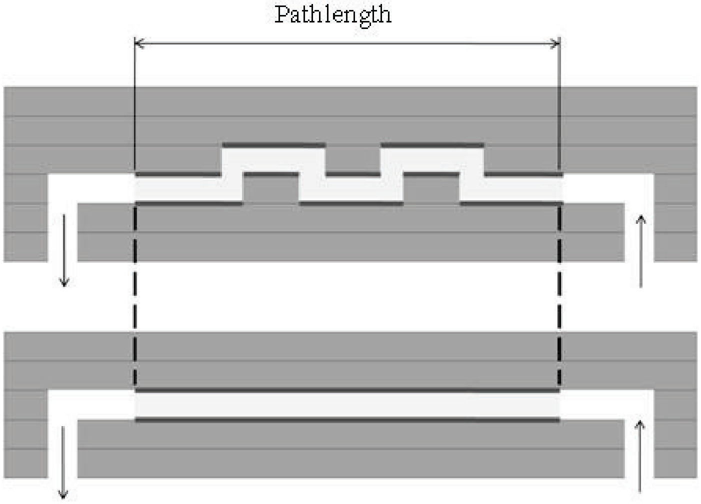

Figure 5. Sectioned side view schematic of the two “channel shape” levels: 3-D (top) and planar (bottom), also illustrating convention used to clarify Path Length for each channel shape

Experimental Setup

In theory, the percent decomposition in Equation 2 of rocket grade hydrogen peroxide is a direct representation of catalyst chamber performance providing the analysis platform for a full factorial experimental design. In order to determine the presence, if any, of un-decomposed hydrogen peroxide in the exhaust plume, the hot gases exiting the catalyst chamber must be captured and then condensed into an aqueous form. When a liquid sample of the chamber exhaust is obtained, it can then be analyzed with a digital refractometer to measure the mass fraction of hydrogen peroxide contained within the sample. A liquid sample of exhaust products containing pure water indicates complete decomposition of the HTP. To ensure a valid comparison of factors, the test prototypes must reach steady state operating conditions prior to sample collection. Obtaining an exhaust sample during the transient start-up phase could yield a highly inaccurate representation of that devices performance and is beyond the scope of this work. As observed in previous tests, the mass fraction of HTP in the exhaust is highly variable during this phase but will eventually plateau when the catalyst chamber reaches a self-sustaining state of operation. The catalyst chamber substrate will also reach a relatively constant temperature during this steady state operation. For this reason, substrate surface temperature will be logged with a Type-K thermocouple and will be used to indicate when a steady state operating condition is achieved.

Test apparatus

Initial hardware was used with an addition to measure the catalyst chamber performance. The original test stand shown in Figure 6 is fabricated primarily from 1/2" Aluminum stock and controlled using a LabVIEW interface, a programmable software package. Featured hardware includes a 20mL Stainless Steel syringe pump capable of supplying HTP propellant to the LTCC device at virtually any flow rate. After the 1/8” SS tubing system is purged via high/low-point bleed valves, the propellant travels through the main shut-off valve where it then passes through the middle of the three small holes located on the vertical plate. Prior to this study, prototype testing was achieved by directly interfacing propellant supply system to LTCC substrates through a Teflon o-ring compression fitting, downstream from the main shut-off valve. Two socket head screws align with the threaded holes on either side of the propellant supply port and tightened by hand until properly sealed. The first generation HTP test stand was designed specifically for the monopropellant LTCC micro-thruster concept and focused primarily on device functionality rather than performance.

The original test stand was modified for retrieval of the above-mentioned data points. The modifications enable the controlling, condensing, and characterizing of catalyst chamber exhaust during operation and are circled in the left hand side of Figure 6. It was designed to integrate with the original test stand without any physical modification thus maintaining its original functionality. The device mounting bracket secures to the test stand through existing fastener connections and interfaces the propellant supply via the existing Teflon o-ring compression connection. A close-up of the mounting bracket connected to the test stand can be seen on the left-hand side of Figure 7.

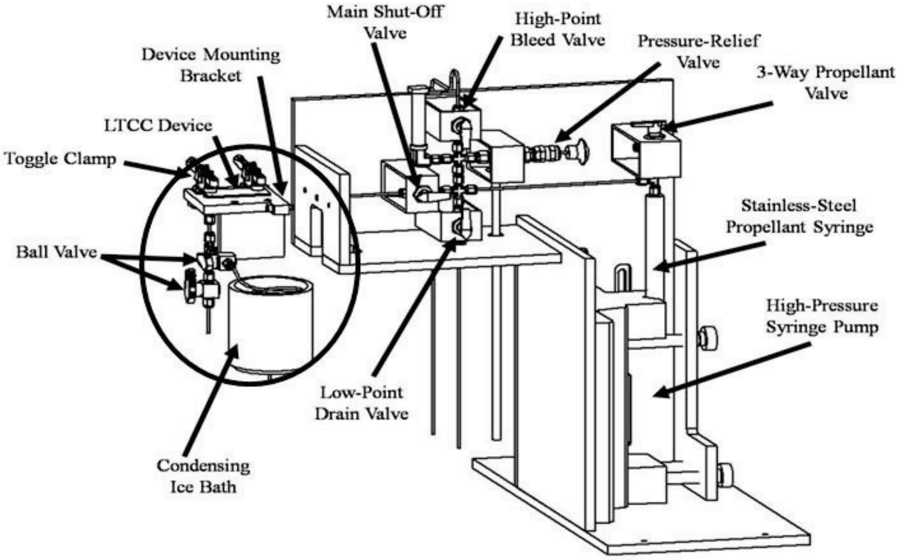

Figure 6. Schematic of HTP test setup

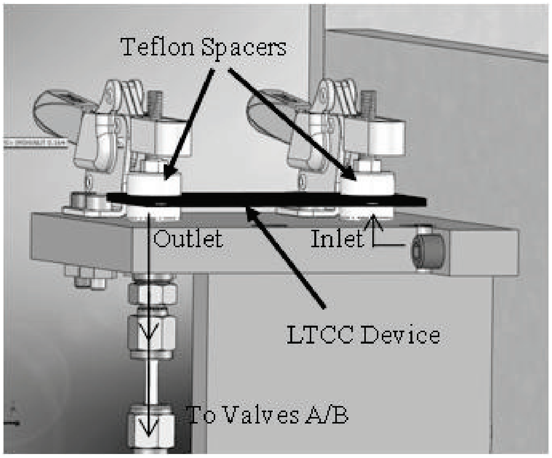

Figure 7. Close-up view of test stand modifications

The Teflon spacers indicated in this figure serve a multi-functional purpose. Teflon's inherently low thermal conductivity provides thermal isolation between test prototypes and the large heat sink associated with the aluminum test stand. In addition to being chemically resistive to hydrogen peroxide, Teflon is an exceptional gasket material for LTCC fluidic connections. Toggle clamps provide a sufficient clamping force to seal the connections between the LTCC device, Teflon spacers, and device mounting bracket. All fittings and the device mounting bracket were cleaned numerous times with isopropyl alcohol to remove any residual hydrocarbons that may decompose hydrogen peroxide outside the catalyst chamber providing an inaccurate sample. After integrating the modifications with the test stand, the entire propellant piping network was passivated with nitric acid for 24 hours to protect against corrosion.

Testing procedure

Figure 8 shows a piping schematic of the test stand modifications shown in Figure 6 and used to describe the testing procedure. The two valves labeled "A" and "B", control the flow of exhaust exiting the LTCC catalyst chamber through the 1/8" SS tubing. Before a test run is allowed to initiate, the operator must manually open valve "B" and close valve "A". The initial valve configuration allows the mostly un-reacted liquid to fall into a collection facility once the test begins and the device warms-up. The horizontal and vertical orientation of valves "A" and "B" respectively were chosen purposely to prevent any fluid leaving the catalyst chamber throughout transient operation to enter the ice bath piping system contaminating the sample. The test sequence was initiated by infusing the 20mL SS syringe with 90% HTP from a gravity fed reservoir, not pictured in Figure 6. Propellant was then supplied to the LTCC test device clamped in the horizontal orientation shown in Figure 7 at a flow rate of 1mL/min. This low flow rate was governed by the volume of the syringe pump and the often lengthy "ignition times" of some prototypes. A type-K thermocouple was placed on the top surface at center of the embedded catalyst chamber for every test run. Surface temperature was manually monitored throughout device warm-up.

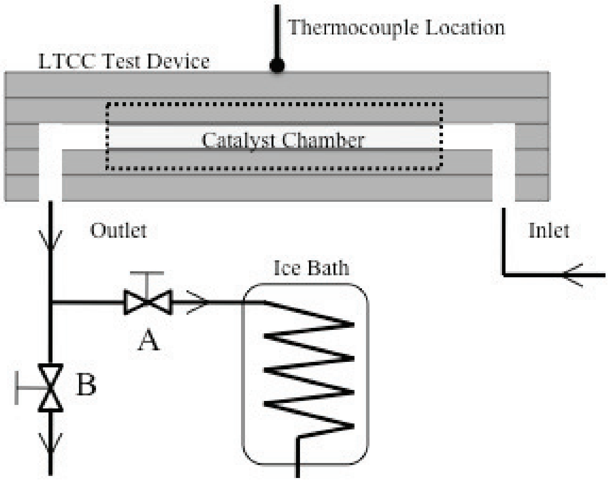

Figure 8. Piping schematic of test stand modifications

Surface temperature was monitored until the device reached a steady value. The test operator recorded the steady state operating temperature and proceeded to open valve "A" followed immediately by the closing valve "B" to direct all exhaust through the coiled tube within the ice bath. There the gaseous mixture condensed into an aqueous solution composed of water and un-reacted hydrogen peroxide. A graduated cylinder collected the condensed sample, which was then analyzed with a digital refractometer to obtain the mass fraction of hydrogen peroxide present in the exhaust sample. This data was then used to calculate the percent decomposition of hydrogen peroxide, the primary data of this study. After completing a test, the stainless steel tubing within the ice bath was flushed several times with DI water to clear out any residual hydrogen peroxide that may contaminate the next sample. The graduated cyclinders used to obtain the condensed exaust sample and digital refractometer were also cleaned with DI water and dried before any subsequent tests were performed.

Test devices

A full factorial experiment was established to investigate the three factors at two levels listed in Table 1. The resulting test matrix is shown in Table 2 and encompasses all combinations of each factor at two levels. Combining factors in this manner will potentially provide a valuable understanding a factor's level of influence on the measured response, decomposition of hydrogen peroxide. A sample size of eight devices is reasonable considering the resource limitations. The nomenclature listed in the rightmost column of Table 2 classifies each configuration and clearly indicates the level of each factor in a fairly straightforward manner. Hyphens separate the three factors and corresponding values. For example, the reference nomenclature for configuration number six is "3D-C2-L20", denoting a three-dimensional channel shape, two channels and a twenty millimeter catalyst chamber Path Length. The test matrix denotes eight distinct catalyst chamber designs, fabricated and tested within an LTCC substrate.

Table 2. Full factorial test matrix for three factors at two levels

Configuration	**Channel Shape**	**Number of Channels**	**Path Length (mm)**	**Nomenclature**
1	Planar	2	10	P-C2-L10
2	Planar	2	20	P-C2-L20
3	Planar	6	10	P-C6-L10
4	Planar	6	20	P-C6-L20
5	3-D	2	10	3D-C2-L10
6	3-D	2	20	3D-C2-L20
7	3-D	6	10	3D-C6-L10
8	3-D	6	20	3D-C6-L20

The overall design of each prototype lowers the cost and time to fabricate while maintaining the geometry required to properly interface with the test stand. The design is such that two identical test devices are located within a single LTCC substrate to be fabricated simultaneously. Producing two functional devices in the amount of time typically required for single LTCC device greatly reduces fabrication costs while increasing yield. The two test devices undergo additional processing after firing to be separated resulting with individual test devices. An example test device can be seen in Figure 9, which features the "P-C2-L20" configuration in a transparent view. Note in this figure that all features are symmetric about the center, which is a commonality between all catalyst chamber designs pertaining to this study. The catalyst chamber in this figure is denoted by the dark colored channel surfaces, representing the silver deposited on top and bottom channel surfaces over a 20mm Path Length. Also note in this figure, the inlet and outlet geometry, which is universal to all prototypes.

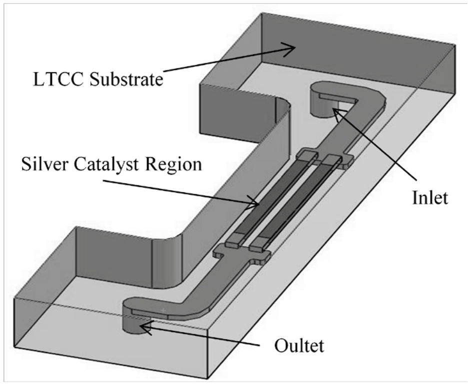

Figure 9. A transparent-isometric view of test device: "P-C2-L20". The silver catalyst (dark grey) deposited on the top and bottom channel surface within the catalyst chamber.

Testing parameters such as overall catalyst chamber volume, propellant flowrate, and channel cross-sectional area are listed in Table 3. The initial flowrate and cross-sectional area values were modeled after previous chamber designs. Initial testing led to mechanical failure of prototypes due to thermal expansion caused by critical amounts of thermal energy released during transient response. A functional prototype design was obtained by greatly reducing the parameters listed in this table as “actual” values. This restricted thermal energy entering the control volume to a manageable level.

Table 3. Initial and actual testing parameters

	Overall Volume (mm^3)	**Propellant Flowrate (mL/min)**	**Cross-Section Channel Area (mm^2)**
Initial	10500	5	1.58
Actual	4050	1	0.79

Results & Analysis

Repeatability & measurement error

The LTCC material system experiences a consistent amount of lateral shrinkage during the firing process and is published by the manufacturer, DuPont. Therefore, any error associated with material shrinkage is minute and can be neglected. In an effort to increase data accuracy, two identical devices were fabricated and tested for the eight configurations outlined by the test matrix.

Testing occurred in a randomized order to reduce any experimental bias. Two samples were harvested from the catalyst chamber exhaust during every experimental test run. With this method, the primary data possessed a maximum standard deviation of 0.058 belonging to the “P-C2-L10” configuration. Based on this value, the experimental data obtained from analyzing condensed exhaust products represents the steady state operating performance particular to the catalyst chamber with reasonable accuracy.

However, the method of obtaining surface temperature data is a potential error source. Experimental temperature data reflects a mean value observed by the experimenter during steady operation. Actual temperatures fluctuated about the recorded mean. The observed fluctuations became large as +/- 10ºC in some cases raising suspicions relating to the accuracy of the recorded value.

Results overview

Test results for all eight configurations are listed in Table 4. The Analysis of Variance technique was employed to analyze the effectiveness of the three factors between low and high values. The factorial experiment was duplicated to improve statistical accuracy. Experimental results show two factors to be a significant influence on the performance while the third factor remains inconclusive.

Table 4. Experimental data for each device and configuration.

	Test Device 1		**Test Device 2**		**Sample Mean**		**St. Dev.**	
Configuration	% Decomp.	Temp (°C)	%Decomp.	Temp (°C)	%Decomp.	Temp (°C)	%Decomp.	Temp (°C)
P-C2-L10	77.8	225	87.2	260	82.5	242.5	6.647	24.75
P-C2-L20	54.3	210	52.6	205	53.5	207.5	1.202	3.536
P-C6-L10	90.0	277	88.1	300	89.1	288.5	1.344	16.26
P-C6-L20	88.5	265	87.5	280	88.0	272.5	0.707	10.61
3D-C2-L10	80.8	255	73.5	200	77.2	227.5	5.162	38.89
3D-C2-L20	96.5	270	92.7	265	94.6	267.5	2.687	3.54
3D-C6-L10	91.6	290	90.3	297	91.0	293.5	0.919	4.950
3D-C6-L20	97.7	275	96.7	290	97.2	282.5	0.707	10.61

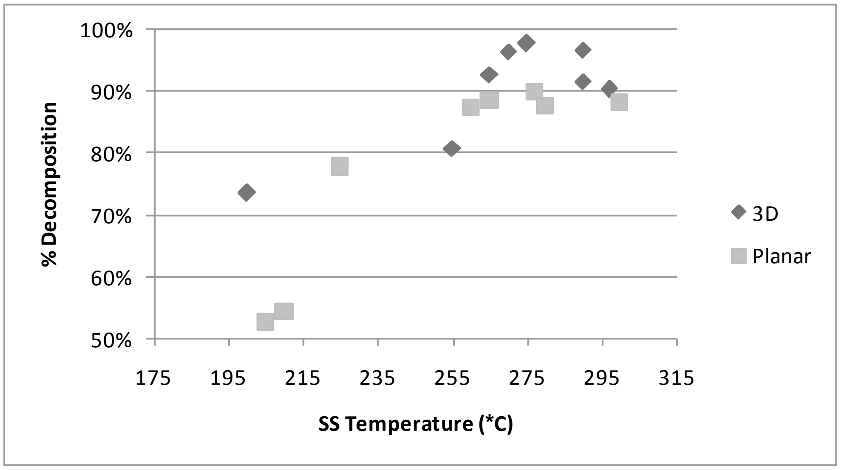

Figure 10. Percent decomposition vs. Steady State Temperature graph for all "3D" and "Planar" configurations.

Experimental data shown in Figure 10 illustrates the influence Channel Shape has on catalyst chamber performance. There is a trend of increasing Percent Decomposition with increasing temperature for both configurations. For temperatures greater than 255°C, several of the 3D configurations approach the maximum decomposition of 100% while the planar configurations do not rise above 90°C. Overall, the planar configurations are the lowest performers.

With the planar design, the fluidic boundary layer along the upper and lower walls is undisrupted. Depleted regions might form near the channel walls in the slow moving boundary layer[3]. The highly laminar boundary layer limits the rate at which un-reacted molecules attach to the silver catalyst. Un-reacted core flow will likely exit the catalyst chamber before it can decompose. Conversely, vertical layer changes are believed to disrupt the boundary layer more effectively. Hydrogen peroxide molecules are more likely to come in contact with a catalyst site resulting in a higher decomposition fraction. Experimental results suggest the 3D channel shape is a highly effective catalyst chamber design. Additionally, this type of fluidic structure highlights the advantages of LTCC making it a desirable material.

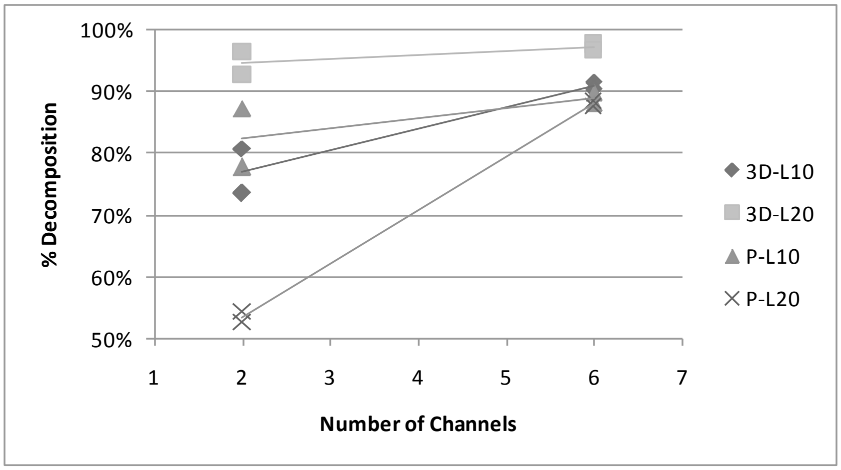

Figure 11. Percent Decomposition vs. "Number of Channels" for all configurations.

The Number of Channels factor also shows a significant influence on catalyst chamber performance, as seen in Figure 11. The graph compares devices containing the same Channel Shape and Path Length combination at their two and six channel states. Each device in Figure 11 demonstrates higher decomposition efficiencies at the

"C6" configuration than the corresponding "C2" design. A smaller spread of variation for the "C6" data is also observed. The largest change occurs for the P-L20 configuration whereas the 3D-L20 has the least change with channel number. Also note that both 3D configurations reach a decomposition percentage better than 90% with the six-channel configuration.

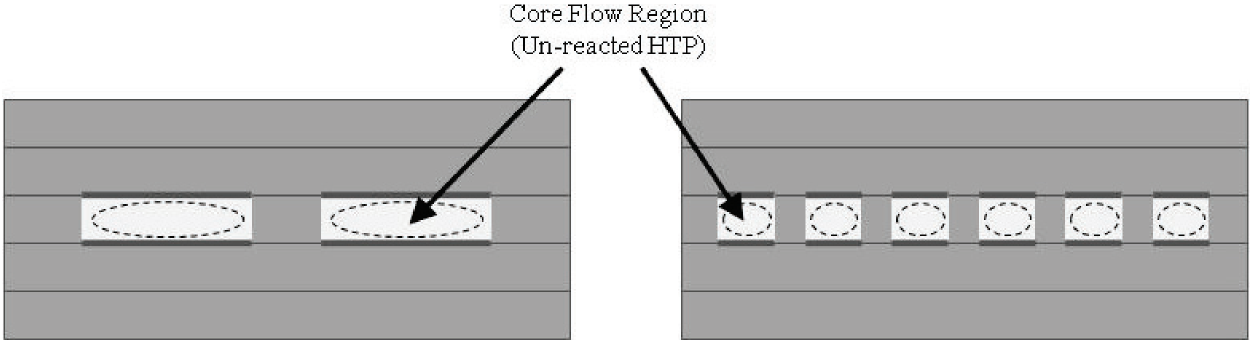

Figure 12. Cross-sectional view of "C2" (left) and "C6" (right) devices depicting the un-reacted core flow regions.

Reducing the hydraulic diameter of an individual channel is believed to improve the catalyst chamber performance. Fundamentally, it reduces the core flow region per channel where un-reacted hydrogen peroxide exists. This is depicted in Figure 12 with cross-sectional views of the two and six channel devices. The larger channels belonging to "C2" have more volume for un-reacted hydrogen peroxide to exist. The larger core flow tends to move through the channels without as much mixing as the "C6" configuration. Additional sidewalls cause additional mixing that allows more core flow to reach the catalyst surface thus improving the reaction and the balance of energy crossing the control volume boundary.

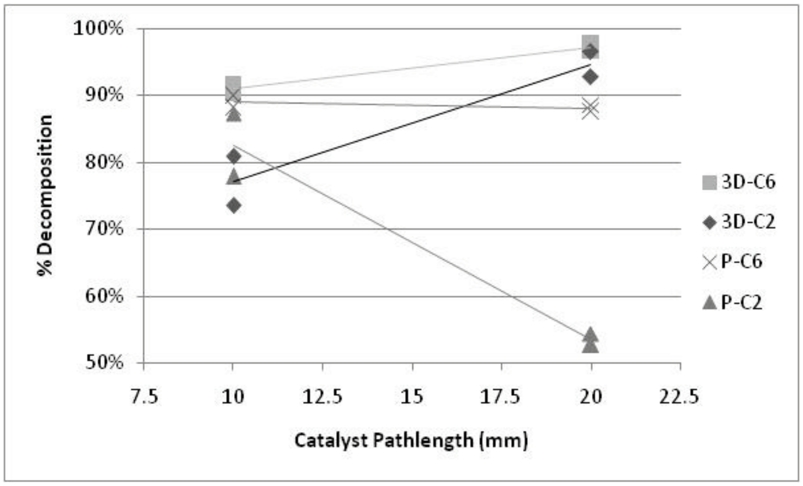

Figure 13. Percent Decomposition vs. "Catalyst Chamber Path Length" for all configurations

Figure 13 analyzes the Path Length factor in a manner similar to that of Figure 11. The experimental data presented in this graph suggest longer Path Lengths improve the performance of both 3D devices. The "P-C6" configuration performs slightly worse with a 20mm Path Length, while "P-C2" appears to perform much worse with the longer Path Length. However, an error in fabrication of the "P-C2-L20" device may have occurred resulting with the low performance. The contradicting behavior between 3D and Planar configurations in this figure suggests the possibility of an optimal length. Further investigation on this factor is left for future work. A qualitative effort has been made to interpret the data in Figure 13. One possible explanation takes into account the heat of reaction spreading throughout the device due to the high thermal conductivity of silver.

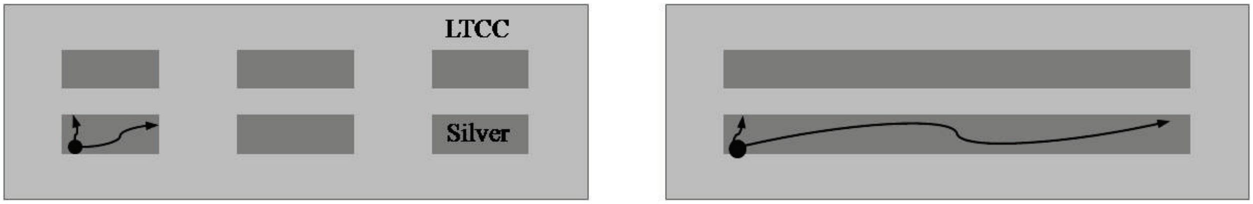

Figure 14. Top view of “3D” (left) and “Planar” (right) of silver catalyst
embedded on the LTCC surface of the catalyst chamber layer.

Catalyst chamber performance will degrade as heat loss increases. Depending on the configuration, the silver catalyst is thought to promote or retard the heat of reaction conducting into the substrate, due to silver being 130 times more thermally conductive than LTCC. This is particularly the case for Planar catalyst chambers with silver deposited on a single layer of LTCC. The continuous silver material inherent to Planar configurations provides a highly conductive path to spread heat quickly throughout substrate. Illustrated in the right side of Figure 14 is a top view schematic of the “P-C2-L20” configuration. The low performance demonstrated by this configuration could be attributed to the large thermally conductive paths promoting heat loss. Similarly, improvement in 3D catalyst chamber performance is believed to be characteristic of the silver “islands” illustrated on the left side of Figure 14. Surrounded by LTCC, reaction heat is confined to the small silver regions embedded on a single layer of LTCC.

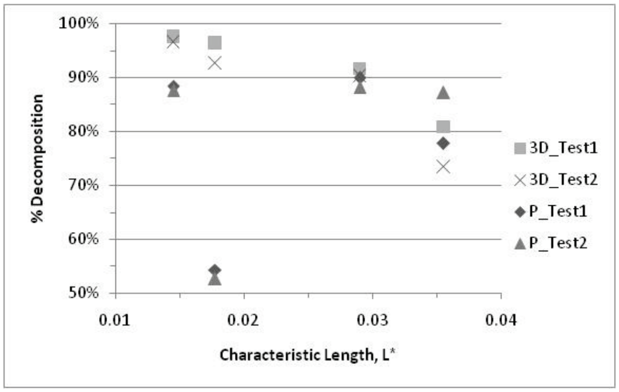

Figure 15. Non-dimensionalized graph depicting % decomposition vs. the characteristic channel
length data for tests 1 and 2 for all “3D” and “Planar” configurations

To better capture the channel geometry effects, a non-dimensional characteristic length is defined according to equation (3). Where L* is the characteristic length, L is the catalyst path length and D_h is the hydraulic channel diameter for a single channel. For the rectangular cross-sections inherent to fluidics in LTCC, D_h for this study is defined in equation (4). Where the wetted area, $A = w_c h$, is the product of the individual channel width and height; and the wetted perimeter, $P = 2(w_c + h)$.

$$L^* = D_h/L \tag{3}$$

$$D_h = 4A/P = 2w_c h/(w_c+h) \tag{4}$$

An interesting trend is obtained in the non-dimensional plot of Figure 15 containing percent decomposition vs. the characteristic length. The two data points in the 50-60% decomposition range belong to the “P-C2-L20” configuration and are an obvious outlier to this trend. Catalyst chamber prototypes can become defective due to a wide range of fabrication anomalies. These two points are 20% lower than any other data set and indicate an issue with the two identical devices. It is therefore reasonable to discard the "P-C2-L20" data set without drastically affecting the previous results.

Neglecting those points, better decomposition is achieved with both Planar and 3D devices as the value of L* becomes lower. This can occur as a result of longer Path Lengths or smaller hydraulic diameter. Longer Path Lengths would increase the propellant dwell time allowing more decomposition to occur. Also, small D_h might promote fluidic mixing as a result of a higher core flow velocity. This trend indicates a geometric relationship directly related to L* that appears to be configuration independent based on this data.

Statistical analysis

Statistical analysis of the experimental data reveals the significance of the three factors. Channel Shape and Number of Channels are highly significant factors influencing catalyst chamber performance due to the low p-values of 0.0213 and 0.0517, respectively. Catalyst Path Length possessed a relatively high p-value of 0.7706, rendering it inconclusive and again suggests an optimal length. Additional duplication of the experiment is necessary to increase statistical significance of the results.

Concluding Remarks

A full factorial experiment was created to investigate various channel characteristics believed to influence the performance on a catalyst chamber embedded in LTCC. Three factors were chosen based on previous work and varied between two distinct levels, resulting with eight test configurations. Initial tests emphasized the importance of thermal management on LTCC microthruster design as in larger engines, such as the Space Shuttle Main Engine. Experimental results emphasize the effectiveness three dimensional fluidic structures have on catalyst chamber performance. This result indicates key advantages of the LTCC material system for similar applications. Secondly, smaller channels have been determined to improve catalyst chamber performance for Planar or 3D configurations. Also, Catalyst Path Length was determined to be inconclusive with a high p-value. Lastly, an interesting geometric trend independent of configuration was observed by analyzing the characteristic channel length and lead to the discovery of a defective prototype creating an outlier in the data set.

Experimental results are still being considered at this time. Additional repetitions of the experimental test matrix are required to improve statistical significance of the data. The test matrix will be expanded to encompass mid-range values of the Number of Channels and Catalyst Path Length factors. This will provide a better understanding of a factor's effectiveness on catalyst chamber performance. The mid-range Path Length values will also indicate the presence of any optimal length.

References

[1] Micci, M.M. and A.D. Ketsdever, *Micropropulsion for small spacecraft*. Progress in astronautics and aeronautics, v. 187. 2000, Reston, Va.: American Institute of Aeronautics and Astronautics.

[2] Hitt, D., C. Zakrzwski, and M. Thomas, *MEMS-based satellite micropropulsion via catalyzed hydrogen peroxide decomposition.* SMART MATERIALS AND STRUCTURES, 2001. 10(6): p. 1163-1175.

[3] Plumlee, D., J. Steciak, and A. Moll, *Development and Simulation of an Embedded Hydrogen Peroxide Catalyst Chamber in Low-Temperature Co-Fired Ceramics.* International Journal of Applied Ceramic Technology, 2007. 4(5): p. 406-414.

[4] Plumlee, D., J. Steciak, and A. Moll. *Development of a Monopropellant Micro-Nozzle and Ion Mobility Spectrometer in LTCC*.

[5] Kuan, C., G. Chen, and Y. Chao. *Development of a High Test Hydrogen Peroxide (HTP) Micro-Thruster*.

[6] Platt, D. *A Monopropellant Milli-Newton Thruster System for Attitude Control of Nanosatellites*. 2002.

[7] Rusek, J.J. *Future of hydrogen peroxide for space propulsion and power applications*. in *Proceedings of the First International Conference on Green Propellants for Space Propulsion*. 2001. Noordwijk, Netherlands: European Space Agency.